Late Quaternary stratigraphy of western Yamal Peninsula, Russia: New constraints on the configuration of the Eurasian ice sheet

Steven L. Forman* Department of Earth and Environmental Sciences, University of Illinois, Chicago, Illinois 60607-7059, USA
Ólafur Ingólfsson Earth Sciences Center, Göteborg University, Box 460, Göteborg S-405 30, Sweden
Valery Gataullin Oil and Gas Research Institute, Riga, LV 1006, Latvia
William F. Manley Institute of Arctic and Alpine Research, University of Colorado, Boulder, Colorado 80309-0450, USA
Hanna Lokrantz Earth Sciences Center, Göteborg University, Box 460, Göteborg S-405 30, Sweden

ABSTRACT

Ice-sheet reconstructions for the last glacial maximum in northern Eurasia range from nearly complete coverage by a contiguous marine-based ice sheet to large unglaciated areas. Stratigraphic records from Yamal Peninsula, Russia, provide new insight on the eastern limit of the Eurasian ice sheet in the Kara Sea. Radiocarbon and infrared stimulated luminescence ages from coastal cliff sections date the emplacement of the Kara diamicton as older than ca. 40 ka, reflecting regional glaciation. Ice-wedge growth, peat accumulation, and eolian and fluvial deposition characterized the past ~40 k.y. and do not support coverage of Yamal Peninsula by an ice sheet or proximity to a glacier margin. Thus, the late Weichselian Eurasian ice sheet was largely confined to Barents Sea and its global sea-level contribution is reduced to ~7 m of sea-level equivalent.

INTRODUCTION

Large uncertainties remain on the extent and thickness of the last ice sheet over the extensive shallow shelves bordering northern Eurasia. Glacial-maximum ice-sheet reconstructions range from nearly complete coverage of northern Russia by a contiguous marine-based ice sheet (Lambeck, 1995; Peltier, 1996; Grosswald, 1998) to individual ice caps centered on arctic archipelagos that advanced onto adjacent shelves (Velichko et al., 1997). The maximum discrepancy between ice-sheet reconstructions is equivalent to about 14 m of global sea level. Hence, the existing uncertainty in past ice-sheet volume confounds efforts to balance eustatic sea-level lowering with global models of past ice-sheet volume (Peltier, 1996) and advance predictions of future sea level (Peltier, 1988).

The presence of glacial flutes and till in the central Barents Sea provides unambiguous evidence for a grounded ice sheet on the Barents Sea shelf during the late Weichselian (Solheim et al., 1990). This ice sheet inundated adjacent Svalbard (Landvik et al., 1998) and expanded northward to the continental shelf edge, filling the 500+ m deep Franz Victoria and Saint Anna troughs (Lubinski et al., 1996; Polyak et al., 1997). Studies of postglacial emergence indicate maximum ice-sheet loading over the central Barents Sea and eastern Svalbard (Forman et al., 1997). This isostatic response within prescribed glacier limits and coupled with refinements in modeling Earth rheology is the basis for reconstructing a 2-km-thick ice sheet over the Barents Sea (Lambeck, 1995; Peltier, 1996). However, there are few chronologically constrained glacial geologic data to define ice-sheet limits east of Novaya Zemlya, confounding reconstructions of late Quaternary ice sheets in northern Eurasia. We initiated field research on the western Yamal Peninsula (Fig. 1) to address specifically if this area was covered by a 2–3-km-thick ice sheet, as proposed by many ice-sheet reconstructions (Lambeck, 1995; Peltier, 1996; Grosswald, 1998), or remained largely unglaciated during the past ~30 k.y. (Velichko et al., 1997). Here we present new stratigraphic records with conventional and accelerator mass spectrometry radiocarbon ages[1] and infrared stimulated luminescence (IRSL) ages that give needed insights on the late Quaternary extent of the Eurasian ice sheet.

STRATIGRAPHIC AND CHRONOLOGIC CONTROL

The coastal cliff sections of the western Yamal Peninsula contain a rich record of late Quaternary environmental change. Previous studies have documented the continuity of lithostratigraphic units and the glacier origin of the much of the ground ice (Kaplyanskaya and Tarnogradsky, 1986; Gataullin, 1988; Astakhov et al., 1996). Our field studies concentrated on the well-exposed sections in 10–25-m-high coastal cliffs within 5 km south of the Marresale Polar Station (Figs. 1C and 2).

Regional glaciation is signified by the >20-m-thick Kara diamicton and associated kilometer- to meter-scale glaciotectonism. This diamicton has a sheet-like geometry and occurs widely on western Yamal Peninsula south of 71°20′N (Gataullin, 1988). Below the Kara diamicton, tens to hundreds of meters of the middle to late Pleistocene Marresale formation and Labsuyakha sand are deformed, resulting in numerous large (≥10 m) close to isoclinal and recumbent to gently inclined folds. Parallel and harmonic-like folds are present, but most conspicuous are large (hundreds of meters wide) overturned chevron folds. Close to the Marresale Station, the folds are often strongly asymmetrical, with uniform vergence toward the north to northeast, indicating deforming thrusts out of the southern Kara Sea.

The lowermost facies of the Kara diamicton is a stratified diamicton formed by intense shearing, folding, and dislocation of underlying sediments, which have destroyed primary bedding. Sediment shearing is recognized by tightly spaced low-angle thrust faults, recumbent folds, small-scale boudinage structures, shear bands, disharmonic and intrafolial folds, and overturned and truncated silt and sand beds. At a larger scale, the Labsuyakha sand is displaced meters upward into the Kara diamicton, sheared along thrust faults, and tens of meters wide blocks are dislocated and deposited as intraclasts in the Kara diamicton. The Kara diamicton above the zone of subglacial deformation is massive and includes debris-rich ice. The ice can constitute as much as 80% of the diamicton and often has a layered appearance caused by alternating debris bands and ice. Recumbent folds and low-angle thrusts defined by debris bands in the ice show flow toward the northeast, confirming directions indicated by subdiamicton deformations. The massive diamicton facies is a mixture of grain sizes, but the most prominent feature is the random distribution of pebbles. The few cobble-sized clasts are angular or subangular, and frequently have bullet-nose form and glacial striae. Provenance of the matrix and clasts shows enrichment in Paleozoic shale, sandstone, and limestone, originating from Novaya Zemlya, and Cretaceous and Paleogene silt and clay derived from the Kara Sea (Gataullin, 1988). The ice-diamicton complex is interpreted as relict debris-rich glacier ice, preserving glaciodynamic structures. Allochthonous terrestrial organic matter from the underlying Labsuyakha sand and the Kara diamicton yield ^{14}C ages ranging from >26

*E-mail: SLF@uic.edu.

[1]GSA Data repository item 9971, Radiocarbon ages for Quaternary stratigraphic units on western Yamal Peninsula, Russia, is available on request from Documents Secretary, GSA, P.O. Box 9140, Boulder, CO 80301, editing@geosociety.org, or www.geosociety.org/pubs/drpint.htm.

Data Repository item 9971 contains additional material related to this article.

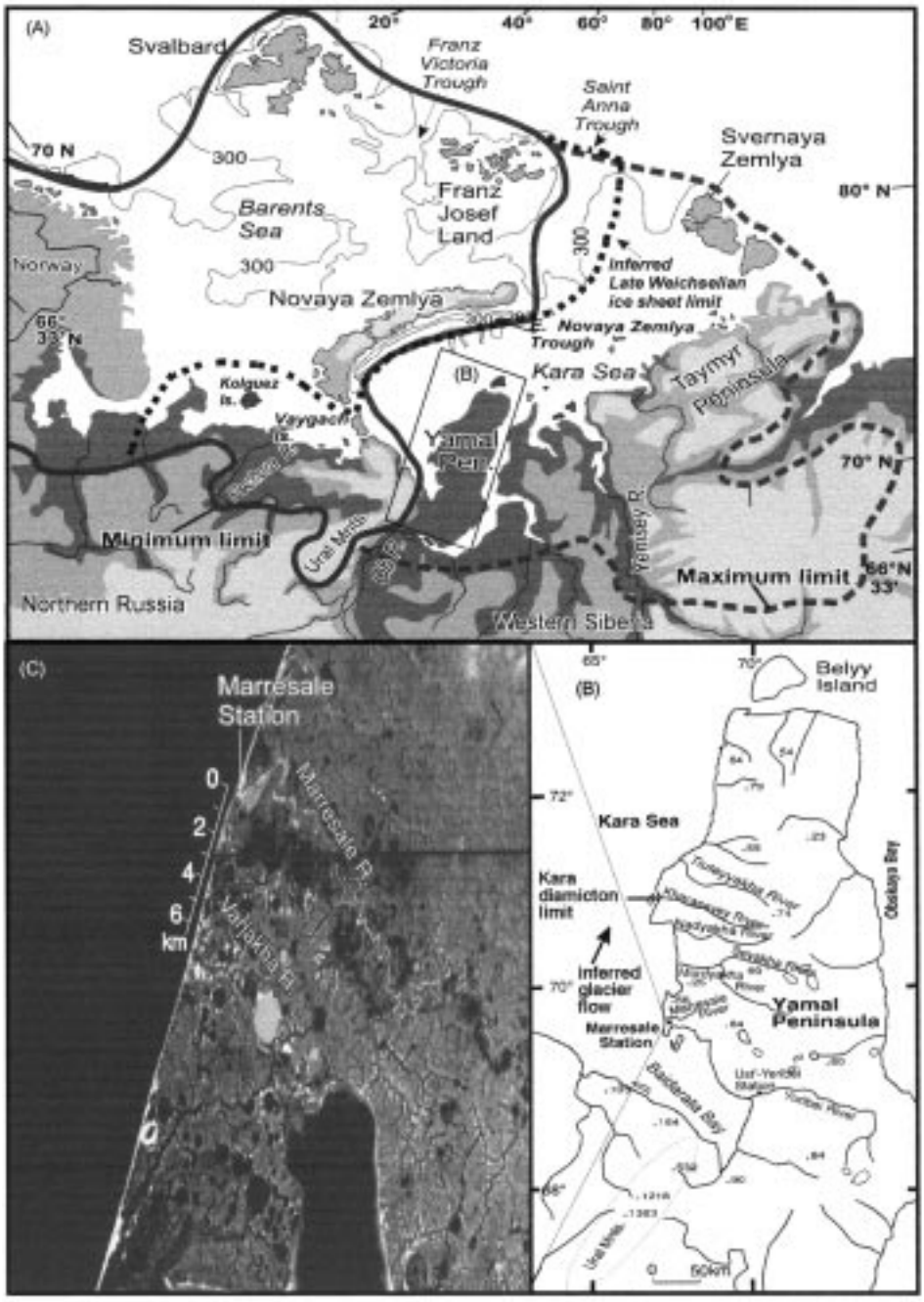

Figure 1. A: Northern Eurasia showing maximum and minimum reconstructed ice-sheet limits of Lambeck (1995) and our inferred late Weichselian limit. Limit north of Kolguez Island is from Svendsen et al. (1999). B: Yamal Peninsula showing major rivers and spot elevations (meters). C: Enlargement of Corona Satellite images 054 050 and 054 051 of western Yamal Peninsula, Russia, taken on September 8, 1964. Kilometer-scale bar shows location of studied sections.

to >55 ka; these are considered minimum limiting ages for this glaciation (Fig. 2).

The Varjakha peat and silt infills 5–20-m-wide basins on the upper surface of the Kara diamicton. This deposit is characterized by alternating centimeter-scale beds of sandy silt and peat, deposited in a shallow lacustrine environment. Individual peat plants from the Varjakha peat and silt yielded ^{14}C ages of 32.4–28.6 ka (Fig. 2) and corresponding fine-grained polymineral extracts gave IRSL ages of 36.0 ± 3.0 (UIC-648), 40.8 ± 4.2 (UIC-650), and 44.0 ± 4.0 (UIC-651) ka, indicating that the ^{14}C ages are finite. The age difference between the two geochronometers is consistent with ^{14}C time-scale calendar calibration (Kitigawa and Van der Plicht, 1998). The Oleny sand, which conformably overlies the lacustrine sediments, is a well-sorted fine sand to fine sandy silt with centimeter-scale subhorizontal and undulatory stratification of eolian origin. Bedding in the Oleny sand is graded; top finer grained laminae exhibit a diffusive lower boundary and contain in situ rooted vascular plant remains that indicate repeated brief periods of subaerial exposure. Syngenetic and en echelon stacked frost-crack pseudomorphs that locally deform bedding and terminate at fine beds attest to active cryogenesis with eolian deposition. Near the top of the Oleny sand, abundant cryogenic convolutions are associated with a horizon of buried ice wedges that represents a significant period of subaerial exposure. Well-preserved vascular plant fragments from the Oleny sand yield ^{14}C ages of 28.2–26.2 ka (Fig. 2); corresponding IRSL ages are 32.8 ± 3.1 ka (UIC-649) and 30.0 ± 3.1 ka (UIC-653), and indicate that the ^{14}C ages are finite.

The upper part of the stratigraphic sequence contains interfingering eolian and fluvial sediments, referred to as the Baidarata sand (Fig. 2). The eolian facies has attributes similar to those of the Oleny sand. Fluvial interbeds usually exhibit horizontal to low-angle stratification, contain pebble- to cobble-size peaty intraclasts, and have an erosive, wavy basal contact with eolian sediments. Higher energy fluvial facies are characterized by trough cross-stratified sands with climbing ripples and occasional pebbles. Vascular plant remains from the eolian facies of the Baidarata sand yielded ^{14}C ages between 16.4 and 12.2 ka (Fig. 2). Subfossil birch tree remains (*Betula pendula*) with ^{14}C ages of ca. 8.9–8.0 ka are rooted into the top of the Baidarata sand and are subsumed by overlying the Nenets peat. The Nenets peat formed between 8 and 1 ka, infills depressions (<7 m deep) on the top of the Baidarata sand, and is buried by discontinuous cover sand, called the Chum sand (Fig. 2)

LATE QUATERNARY ICE-SHEET LIMITS

The pervasive and large-scale glacial tectonism associated with the Kara diamicton and provenance of erratics reflect north to northeasterly glacier flow onto Yamal Peninsula from source areas over Novaya Zemlya and the Kara Sea. However, the configuration of the ice sheet that deposited the Kara diamicton is unresolved. Glaciological modeling indicates that the Saint Anna and Eastern Novaya Zemlya troughs were barriers for the eastward movement of the Barents Sea ice sheet, the majority of flow having been constrained to the troughs (D. MacAyeal, 1999, personal commun.). The north to northeast glacier motion inferred from the Kara diamicton may reflect the lateral expansion of a southward-flowing lobate-glacier margin into the southern Kara Sea from source areas on Novaya Zemlya (cf. Gataullin, 1988). However, there may be glacier flow contribution from southern sources, potentially from the Ural Mountains. Radiocarbon ages of ca. 33 ka and corresponding IRSL ages of ca. 40 ka for the Varjakha silt and peat immediately overlying the Kara diamicton provide minimum limiting ages for this glaciation (Fig. 3). The Kara diamicton may be broadly cor-

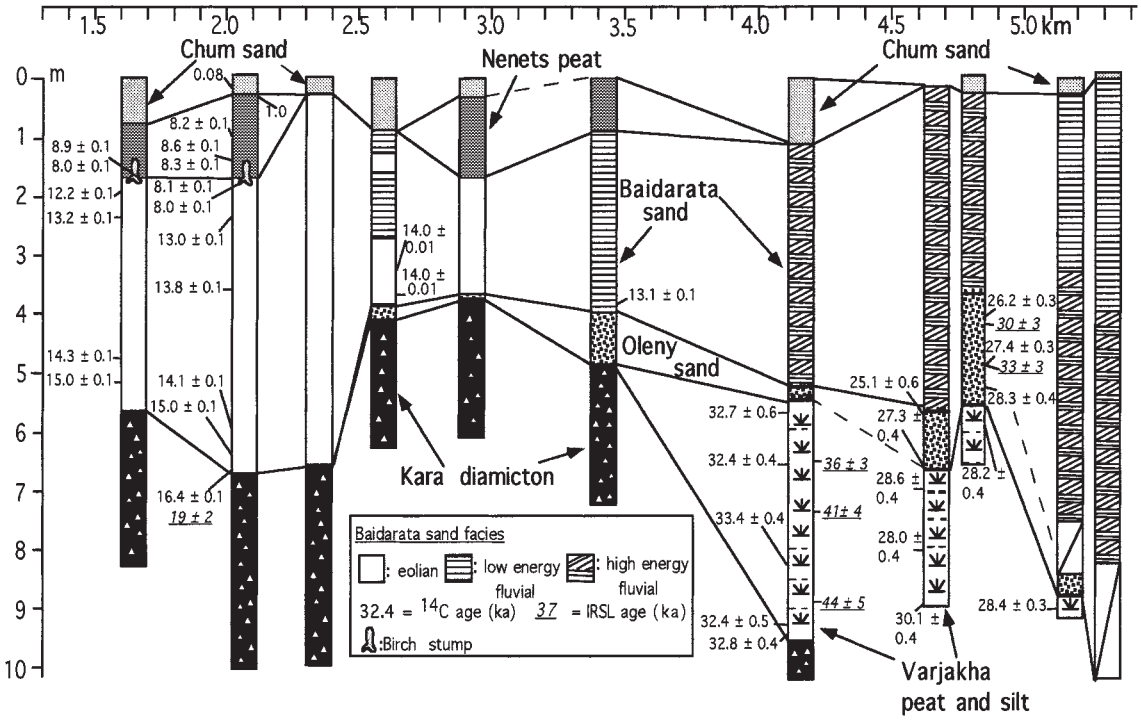

Figure 2. Summary of stratigraphic sections for 4 km of coastal cliff exposures south of Marresale Station showing associated radiocarbon and infrared stimulated luminescence ages (IRSL).

relative with the Markhida till, dated as between >45 and 80 ka in the Pechora River basin, and may be associated with an extensive early Weichselian glaciation in Siberia (Mangerud et al., 1999) and on Svalbard (Mangerud et al., 1998; Forman, 1999). Thus, the Kara diamicton reflects ice-sheet advance across the Yamal Peninsula late in marine oxygen isotope stage 5, stage 4, or earlier, with limits possibly compatible to maximum ice-sheet reconstructions (Lambeck, 1995; Peltier, 1996; Grosswald, 1998).

Field observations and examination of recently declassified Corona Satellite images (3 m resolution) show a clear absence of landforms associated with glacio-isostatic compensation (e.g., raised-beach sequences) on western Yamal (Fig. 1C), which is incompatible with late Weichselian ice-sheet reconstructions that exceed 2 km thickness over the Kara Sea (Lambeck, 1995; Peltier, 1996; Grosswald, 1998). Analysis of the stratigraphic record on western Yamal Peninsula indicates active ice-wedge growth and eolian and fluvial deposition during the late Weichselian, ca. 40–11 ka (Fig. 3). Stratigraphic and geomorphic observations and associated chronologic control do not support coverage of the Yamal Peninsula by a late Weichselian ice sheet or proximity to a glacier margin.

The eastern limit of the late Weichselian Eurasian ice sheet is between Novaya Zemlya and the Yamal Peninsula. Studies on northern Novaya Zemlya document maximum glacio-isostatic emergence between 15 and 10 m and a silty glaciogenic diamicton above the marine limit, evidence for glacial coverage during the late Weichselian (Forman et al., 1999). The diminutive glacio-isostatic response on Novaya Zemlya (<15 m) compared to Franz Josef Land

Stratigraphic Unit	Paleo-environment	Lithology	Uncorrected ^{14}C age (ka)	Infrared Stimulated Luminescence Age (ka)	Inferred Calendar Age (ka)
Chum sand	eolian cover sand		0.08 ± 0.04 "post bomb"		≤ 1.0
Nenets peat	poorly drained upland	ice wedge	1.0 ± 0.04 8.0 ± 0.06 8.0 ± 0.08 8.0 ± 0.06		1.0 to 9.0
Betula horizon	treeline		8.9 ± 0.06 8.1 ± 0.09 8.3 ± 0.06 8.6 ± 0.06		9.0 to 10.0
Baidarata sand	eolian cover sand and low to high energy fluvial		12.2 ± 0.08 13.2 ± 0.08 13.1 ± 0.10 13.0 ± 0.08 13.8 ± 0.08 14.0 ± 0.10 14.1 ± 0.10 14.0 ± 0.10 14.3 ± 0.09 15.0 ± 0.12 15.0 ± 0.10 16.4 ± 0.12	19 ± 2	13 to 20
Oleny sand	eolian cover sand	ice wedge	28.2 ± 0.4 27.4 ± 0.3 28.3 ± 0.4 26.2 ± 0.3 27.3 ± 0.4 25.1 ± 0.6	30 ± 3 33 ± 3	30 to 35
Varjakha peat and silt	shallow lake		32.7 ± 0.6 28.6 ± 0.4 32.4 ± 0.4 28.0 ± 0.4 33.4 ± 0.4 28.3 ± 0.4 32.8 ± 0.4 28.4 ± 0.3 32.4 ± 0.5 30.1 ± 0.4	36 ± 3 41 ± 4 44 ± 5	35 to 45
Kara diamicton	regional glaciation		36.0 ± 0.4 43.1 ± 1.5		60 to 80
Labsuyakha sand Marresale formation	deltaic to shallow marine		>41.9 >26 33.2 ± 0.6 >55.5 >31.5 40.9 ± 1.6 35.1 ± 1.0 35.4 ± 0.3 31.1 ± 0.4 42.0 ± 0.1		>100

Peat silt sand diamicton

Figure 3. Composite stratigraphy, associated radiocarbon and infrared luminescence chronologic control, inferred paleoenvironments, and concluded calendar ages (Stuiver and Reimer, 1993; Kitigawa and Van der Plicht, 1998) for western Yamal Peninsula, Russia.

(20–50 m) indicates modest (<500 m thick) ice-sheet loads near the eastern margin of the Barents Sea ice (Lambeck, 1995; Forman et al., 1999). Marine records from the adjacent Saint Anna trough support early deglaciation and ice-sheet withdrawal from 80°N prior to 13.3 ka (Polyak et al., 1997). Recent marine geologic studies in the southern and northern margin of the East Novaya Zemlya trough document a sequence similar to that identified in the Saint Anna trough, a glacial diamicton covered by deglacial and Holocene marine sediments (L. Polyak, 1998, personal commun.), implying grounding of the Barents Sea ice sheet within this 400 m+ trough. Continuing eastward flow of the Barents Sea ice sheet would be impeded by the Eastern Novaya Zemlya trough, which would funnel flow to the north and the south. Seismic and acoustic surveys immediately northeast of Vaygach Island have identified a 50-m-thick arcuate accumulation of glaciogenic sediments, which may mark the southeastern ice-sheet limit (V. Gataullin, 1998, personal commun.). Thus, we tentatively place the eastern limit of the late Weichselian Barents-Kara Sea ice on the eastern margin of the East Novaya Zemlya trough in the Kara Sea (Fig. 1A).

Our chronologically controlled geomorphic and stratigraphic observations constrain late Weichselian glaciation largely to the Barents Sea; there was limited extension of the ice sheet into the Kara Sea. The inferred ice-sheet configuration (Fig. 1A) is most consistent with the minimum model proposed by Lambeck (1995), with an inferred southern limit north of Kolguez Island (Svendsen et al., 1999). We contend that the Yamal Peninsula and much of Siberia east of the Ural Mountains was distal to moisture sources, evidenced by the prevalence of sand sheets ca. 30–11 ka in the Marresale area. Studies along lowlands of the eastern Kara Sea provide equivocal evidence for coverage by a large ice sheet in the late Weichselian, but support nonglaciation of large areas, and Pleistocene flora, mammals, and humans surviving throughout the late Weichselian into the Holocene (Makeyev et al., 1993; Andreev et al., 1997; Vasil'chuk et al., 1997; Möller et al., 1999). Thus, the late Weichselian glacier extent is characterized by expansion of valley glaciers in the Ural Mountains (Astakhov, 1997) and probably limited extension of ice caps on Severnaya Zemlya (Bolshiyanov and Makeyev, 1995), rather than the large-scale continental glaciation of western Siberia envisioned by many ice-sheet models (Lambeck, 1995; Peltier, 1996; Grosswald, 1998).

Our glacial geologic studies on Yamal Peninsula reduce the global sea-level contributions of ice sheets in the Eurasian north to about 7 m of sea-level equivalent, considerably less than the previous estimates of 16 m (Tushingham and Peltier, 1991). This ice sheet, largely confined to Barents Sea, increases the apparent discrepancy between eustatic sea-level depression and global glacier volume to more than 20 m of global sea-level equivalent at the time of the last glacial maximum (cf. Andrews, 1992). This missing water may partially reside in high Arctic ice caps, ice-sheet growth immediately prior to deglaciation, or reflect limitations in modeling Earth rheology and Quaternary ice sheets.

ACKNOWLEDGMENTS

The National Science Foundation and the Swedish Natural Sciences Research Council supported this study. We thank M. Leibman of the Earth Cryosphere Institute, Moscow, for arranging logistics and the stay at the Marresale Station, and A. Andreev, J. Piotrowski, and E. Domack for reviews.

REFERENCES CITED

Andreev, A. A., Tarasov, P. E., Romanenko, F. A., and Sulerzhitsky, L. D., 1997, Younger Dryas pollen records from Sverdrup Island (Kara Sea): Quaternary International, v. 41-42, p. 135–139.

Andrews, J. T., 1992, A case of missing water: Nature, v. 358, p. 281.

Astakhov, V. I., 1997, Late glacial events in the central Russian Arctic: Quaternary International, v. 41-42, p. 17–25.

Astakhov, V. I., Kaplyanskaya, F. A., and Tarnogradsky, V. D., 1996, Pleistocene permafrost of west Siberia as a deformable glacier bed: Permafrost and Periglacial Processes, v. 7, p. 165–191.

Bolshiyanov, D. Y., and Makeyev, V. M., 1995, The Archipelago Severnaya Zemlya: Glaciation, history and environment: St. Petersburg, Gidrometizdat, 216 p. (in Russian).

Forman, S. L., 1999, Infrared and red stimulated luminescence dating of late Quaternary near shore sediments from Spitsbergen, Svalbard: Arctic, Antarctic and Alpine Research, v. 31, p. 34–49.

Forman, S. L., Weihe, R., Lubinski, D., Tarasov, G., Korsun, S., and Matishov, G., 1997, Holocene relative sea-level history of Franz Josef Land, Russia: Geological Society of America Bulletin, v. 109, p. 1116–1133.

Forman, S. L., Lubinski, D. J., Zeeberg, J. J., Polyak, L., Miller, G. H., Matishov, G. G., and Tarasov, G., 1999, Postglacial emergence and late Quaternary glaciation on northern Novaya Zemlya, Arctic Russia: Boreas, v. 28, p. 133–145.

Gataullin, V. N., 1988, Upper Quaternary deposits of the western coast of the Yamal Peninsula, Russia [Ph.D. thesis]: Leningrad, Russia, Federal Geological Institute, 213 p. (in Russian).

Grosswald, M. G., 1998, Late-Weichselian ice sheets in Arctic and Pacific Siberia: Quaternary International, v. 45, p. 3–18.

Kaplyanskaya, F. A., and Tarnogradsky, V. D., 1986, Remnants of the Pleistocene ice sheets in the permafrost zone as an object for paleoglaciological research: Polar Geography and Geology, v. 10, p. 65–72.

Kitigawa, H., and Van der Plicht, J., 1998, Atmospheric radiocarbon calibration to 45,000 yr B.P.: Late glacial fluctuations and cosmogenic isotope production: Science, v. 279, p. 1187–1190.

Lambeck, K., 1995, Constraints on the Late Weichselian ice sheet over the Barents Sea from observations of raised shorelines: Quaternary Science Reviews, v. 14, p. 1–16.

Landvik, J. Y., Bondevik, S., Elverhoi, A., Fjeldskaar, W., Mangerud, J., Siegert, M. J., Salvigsen, O., Svendsen, J.-I., and Vorren, T. O., 1998, The last glacial maximum of Svalbard and the Barents Sea area: Ice sheet extent and configuration: Quaternary Science Reviews, v. 17, p. 43–75.

Lubinski, D. J., Korsun, S., Polyak, L., Forman, S. L., Lehman, S. J., Herlihy, F. A., and Miller, G. H., 1996, The last deglaciation of the Franz Victoria Trough, northern Barents Sea: Boreas, v. 25, p. 89–100.

Makeyev, V. M., Pitul'ko, V. V., and Kasparov, A. K., 1993, The natural environment of the De Long Archipelago and ancient man in the late Pleistocene and early Holocene: Polar Geography and Geology, v. 17, p. 55–63.

Mangerud, J., Dokken, T., Hebbeln, D., Heggen, B., Ingolfsson, O., Landvik, J. Y., Mejdahl, V., Svendsen, J. I., and Vorren, T. O., 1998, Fluctuations of Svalbard–Barents Sea Ice Sheet during the last 150,000 years: Quaternary Science Reviews, v. 17, p. 11–42.

Mangerud, J., Svendsen, J. I., and Astakhov, V. I., 1999, Age and extent of the Barents and Kara ice sheets in Northern Russia: Boreas, v. 28, p. 46–80.

Möller, P., Bolshiyanov, D. Y., and Bergsten, H., 1999, Weichselian geology and palaeoenvironmental history of the central Taymyr Peninsula, Siberia, indicating no glaciation during the last global glacial maximum: Boreas, v. 28, p. 92–114.

Peltier, W. R., 1988, Global sea level and Earth rotation: Science, v. 240, p. 895–901.

Peltier, W. R., 1996, Mantle viscosity and ice-age ice sheet topography: Science, v. 273, p. 1359–1364.

Polyak, L., Forman, S. L., Herlihy, F. A., Ivanov, G., and Krinitsky, P., 1997, Late Weichselian deglacial history of the Svyataya (Saint) Anna Trough, northern Kara Sea, Arctic Russia: Marine Geology, v. 143, p. 169–188.

Solheim, A., Russworm, L., Elverhøi, A., and Nyland-Berg, M., 1990, Glacial flutes, a direct evidence for grounded glacier ice in the northern Barents Sea: Implications for the pattern of deglaciation and late glacial sedimentation, *in* Dowdeswell, J. A., and Scourse, J. B., eds., Glaciomarine environments: Processes and sediments: Geological Society [London] Special Publication 53, p. 253–268.

Stuiver, M., and Reimer, P. J., 1993, Extended ^{14}C data base and revised CALIB 3.0 ^{14}C age calibration program: Radiocarbon, v. 35, p. 215–230.

Svendsen, J. I., Astakhov, V. I., Bolshiyanov, D. Y., Demidov, I., Dowdeswell, J., Gataullin, V., Hjort, C., Huberten, H. W., Larsen, E., Mangerud, J., Melles, M., Møller, P., Saarnisto, M., and Siegert, M. J., 1999, Maximum extent of the Eurasian ice sheets in the Barents and Kara Sea region during the Weichselian: Boreas, v. 28, p. 234–242.

Tushingham, A. M., and Peltier, W. R., 1991, ICE-3G: A new model of late Pleistocene deglaciation based upon geophysical predictions of post-glacial sea level change: Journal of Geophysical Research, v. 96, p. 4497–4523.

Vasil'chuk, Y., Punning, J.-M., and Vasil'chuk, Y., 1997, Radiocarbon ages of mammoths in northern Eurasia: Implications for population development and late Quaternary environment: Radiocarbon, v. 39, p. 1–18.

Velichko, A. A., Kononov, Y. M., and Faustova, M. A., 1997, The last glaciation of Earth: Size and volume of ice sheets: Quaternary International, v. 41-42, p. 43–52.

Manuscript received February 22, 1999
Revised manuscript received May 14, 1999
Manuscript accepted May 30, 1999